

# EFFECTS OF NON-SINGULAR STRESS TERMS AND BIREFRINGENT COEFFICIENT ON CAUSTICS UNDER VARIOUS FRACTURE MODE LOADINGS

Ouk Sub Lee\*, Min Ku Han\* and Sung Kyung Hong\*

(Received July, 1989)

This report investigates the effect of the first few higher-order, non-singular stress terms and the coefficient of optical anisotropy on the shapes of the initial curves and the caustics in birefringent plates under Mode I and Mode II static loading conditions. For Mode I and Mode II loading conditions, Williams stress function is employed to generate various theoretical initial curves and caustics. Some experimentally obtained double caustics are compared to the theoretically generated double caustics. The agreement is found to be good as far as the shapes of caustics are concerned although it is not easy, if not impossible, to distinguish the effect of each higher-order terms.

**Key Words :** Birefringent Coefficient, Caustics, Higher-Order Terms, Non-Singular Stress Terms, Stress Intensity Factor, Optically Anisotropic Materials, Half Interval Search, Williams Stresss Function

## 1. INTRODUCTION

The optical method of either reflected or transmitted caustics has been successfully used in fracture mechanics investigations. Potentially, this relatively new experimental technique has application into a wide variety of problems, covering static and dynamic crack propagation studies, some elasticity problems, and contact stress analysis in both opaque and transparent materials(Lee and Kwon, 1987; Theocaris and Gdoutos, 1972). However, the above applications of the method of caustics are mostly confined within the limit of elasticity problems.

Especially for linear elastic fracture problems, the stress field at the vicinity of a crack tip was represented only by the singular stress term, i.e., the stress intensity factor(SIF). Then the relationship between the transverse diameter of the caustics( $D_c$ ) and the SIF under Mode I loading condition( $K_I$ ) was found to be  $K_I \propto D_c$ (Kalthoff, 1987). Recently Theocaris and Ioakimidis(1979) studied the effect of non-singular stress field on the size and shape of the caustics for optically isotropic materials. Phillips and Sanford(1981) extended the similar study into the optically anisotropic materials and found that the transverse diameters of the inner and outer parts of the double caustics had an average value essentially equal to the transverse diameter of the single caustics of optically isotropic material having the same optical constant.

This paper is further extending the study of Phillips and Sanford(1981) by taking the variation of the initial curve into consideration. Furthermore the change of shapes of caustics and initial curves under Mode II and mixed Mode loading conditions associated with higher-order terms were also systematically investigated. The Williams stress function was utilized and the effect of optically anisotropic coefficient( $\xi$ ) was also incorporated(Williams, 1957).

## 2. THEORETICAL

When a light ray transmits a transparent specimen plate of thickness  $t$ , the initial point  $P$  is mapped at a point  $P'$  on the screen located  $Z_0$  away from the specimen as shown in Fig. 1.

The above transformation in Fig.1 may be represented by Kalthoff(1987).

$$\vec{r}' = M \vec{r} - Z_0 \text{grad}(\Delta S) \quad (1)$$

where

- $M$  = magnification factor
- $Z_0$  = distance between specimen and screen
- $\Delta S$  = optical path length change  
 $= Ct [(\sigma_1 + \sigma_2) \pm \xi(\sigma_1 - \sigma_2)]$  (2)
- $C$  = elasto-optic material constant
- $\sigma_1, \sigma_2$  = principal stresses in the plane of the specimen
- $\xi$  = optical anisotropic constant  
 $(=0$  for optically isotropic materials)  
 $(\neq 0$  for optically anisotropic materials)  
 $(=0.223$  for used Polycarbonate specimens under the plane stress condition)

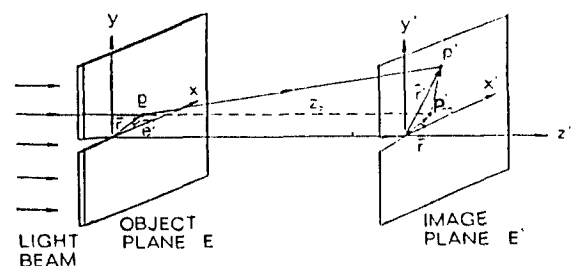


Fig. 1 Geometry for the method of caustics

\*Department of Mechanical Engineering, Inha University, Incheon 402-751, Korea

An optical singular phenomenon occurs in the transformation of  $\vec{r}$  to  $\vec{r}$  whenever the Jacobian  $J(r, \theta)$  of the transformation vanishes, that is, a caustics is generated.

$$J(r, \theta) = 0 \tag{3}$$

corresponds to the caustics determined by the substitution of  $J(r, \theta) = 0$  into the Eq. (1)

The stress distribution surrounding a crack tip under Mode I, Mode II or mixed Mode loading condition may be represented by using Williams stress function(Williams, 1957). The polar stress components derived from the Williams stress function under mixed Mode loading condition may be represented as

$$\begin{aligned} \sigma_r(r, \theta) = & r^{-1/2} [A_1 f_1(r, \theta) + B_1 g_1(r, \theta)] \\ & + A_2 [f_2(\theta) + g_2(\theta)] \\ & + r^{1/2} + [A_3 f_3(r, \theta) + B_3 g_3(r, \theta)] \\ & + r + [A_4 f_4(\theta) + B_4 g_4(\theta)] \\ & + r^{3/2} + [A_5 f_5(r, \theta) + B_5 g_5(r, \theta)] \\ & + r^2 + [A_6 f_6(\theta) + B_6 g_6(\theta)] \end{aligned} \tag{4}$$

$$\sigma_\theta(r, \theta) = F(r, A_1, A_2, A_3, A_4, A_5, A_6, B_1, B_2, B_3, B_4, B_5, B_6) \tag{5}$$

$$\tau_{r\theta}(r, \theta) = G(r, A_1, A_2, A_3, A_4, A_5, A_6, B_1, B_2, B_3, B_4, B_5, B_6) \tag{6}$$

where

- $(r, \theta)$  = polar coordinate at a crack tip
- $A_1, A_2, \dots$  = constants
- $B_1, B_2, \dots$  = constants
- $f_1, f_2, \dots$  = arbitrary functions
- $g_1, g_2, \dots$  = arbitrary functions

It can be shown that the sum and difference of the principal

stresses take in the form, respectively.

$$\sigma_1 + \sigma_2 = \sigma_r + \sigma_\theta \tag{7}$$

$$\sigma_1 - \sigma_2 = \sqrt{(\sigma_r - \sigma_\theta)^2 + 4\tau_{r\theta}^2} \tag{8}$$

Substituting equations (7) and (8) into equation (1), we obtain the equation of caustics. The initial curve,  $r$ , associated with caustics for optically isotropic materials may be obtained such that

$$r = (1.5A_1M^{-1}ClZ_0)^{2/5} \tag{9}$$

under Mode I and with singular term  $A_1$  only.(Note : SIF is imbedded in  $A_1$ )

The introduction of the higher-order terms, mixed mode loading conditions and optical anisotropy into the stress field around the crack tip complicates the governing image equations, and thus does the initial curve equations.

The closed form solutions for both the initial curve and the caustics may not be obtainable. A numerical technique such as the half interval search(Hornbeck, 1975) was used to determine initial curve by making

$$J(r, \theta) \approx 0 \tag{10}$$

The half interval search technique was found to be suitable to solve Eq.(10) since equation did not have troublesome tangent points and it was possible to easily locate an approximate rough root. A flow-chart for this algorithm is shown in Fig. 2.

The  $r_s$  satisfying equation (10) were substituted into equation (1) to obtain corresponding points on the caustics.

### 3. RESULTS AND DISCUSSIONS

As a reference, inner and outer initial curves and caustics were generated with singular term only. Figure 3(a,b) shows theoretically generated caustics and initial curves together with corresponding reference caustics and initial curves under Mode I and Mode II loading conditions, respectively. Fig. 4(a, b) shows the effect of the first non-singular term,  $A_2$ , which is denoted by  $\sigma_{ox}$  in Kobayashi and Ramulu(1981) on both the initial curves and caustics under Mode I loading condition. It is interesting to note that a transition region in terms of the magnitude of  $A_2$  exists for the variation of the transverse diameter( $D_t$ ) of the caustics regardless of the sign of  $A_2$ . The effect of  $A_3$  on both the initial curves and caustics is shown in Fig. 5(a, b). It is noted that the transition region dominates beyond a critical magnitude of  $A_3 = K_f$ . It is found that the inner  $D_t$  becomes bigger with increase of absolute value of  $A_2$ . On the contrary, the outer  $D_t$  has opposite tendency with the growth of  $A_2$ . Therefore, the average of the inner  $D_t$  remains constant irrespective of the sign of  $A_2$  as shown in Fig. 4(a, b) with dashed line.

However, the compensation phenomenon(appeared for  $A_2$ ) does not occur in the case of  $A_3$ . Both the inner and the outer  $D_t$  increase and decrease corresponding to the positive and negative  $A_3$ , respectively. The same characteristic as that of  $A_2$  is found for  $A_4$ . The higher-order terms  $A_5$  and  $A_6$  have the same influence on the caustics as that of  $A_3$ . Figure 6 shows the lower bound of various higher-order terms affecting shape of caustics under Mode I loading condition.

For the Mode II loading condition, the lower bound of

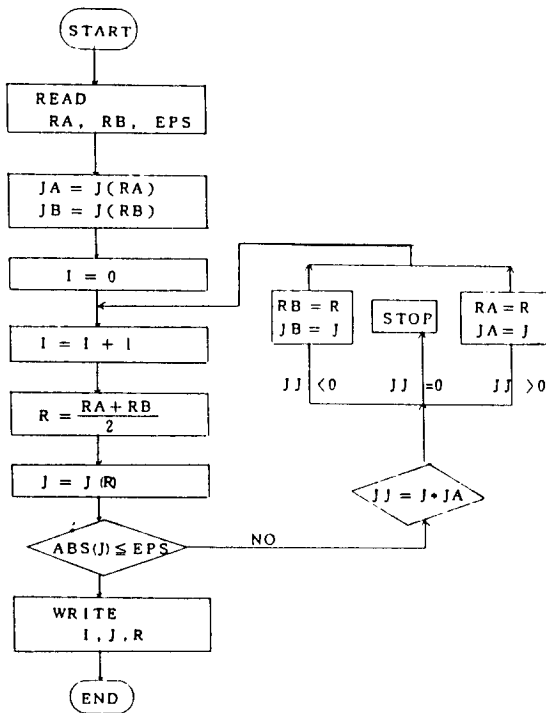


Fig. 2 Flow-chart for the determination of  $J(r, \theta) = 0$

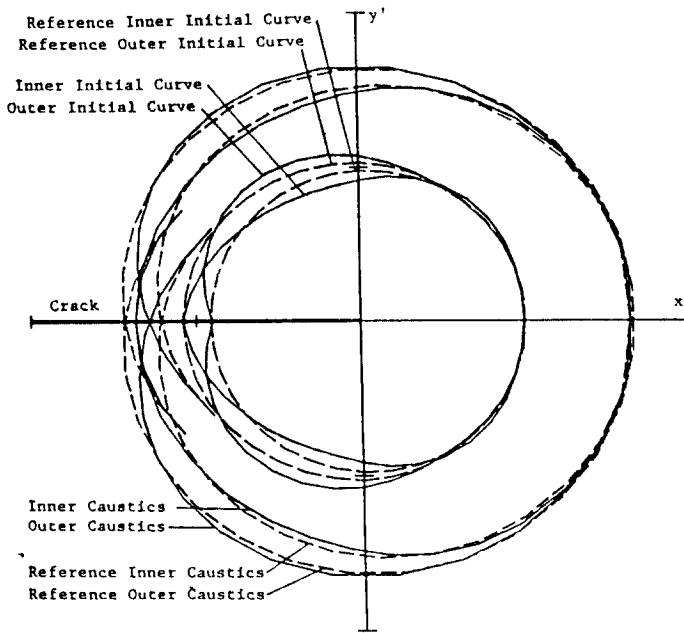


Fig. 3 (a) Theoretically generated Mode I double caustics ( $A_2 = -10K_1$ )

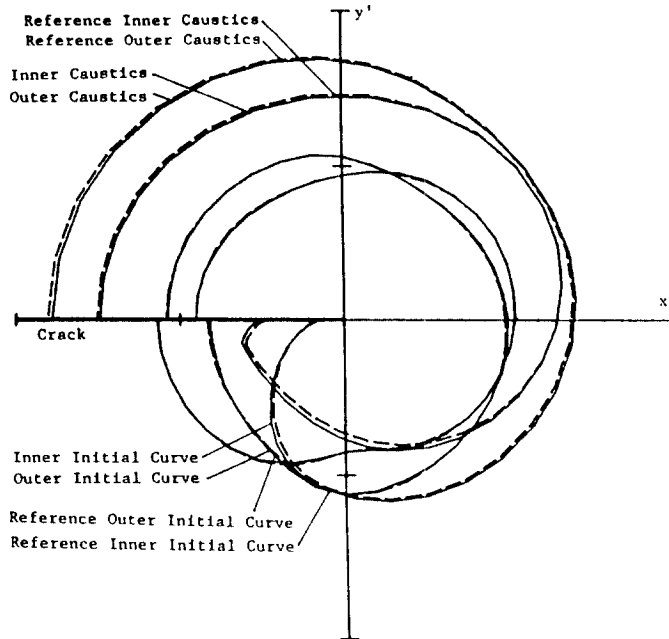
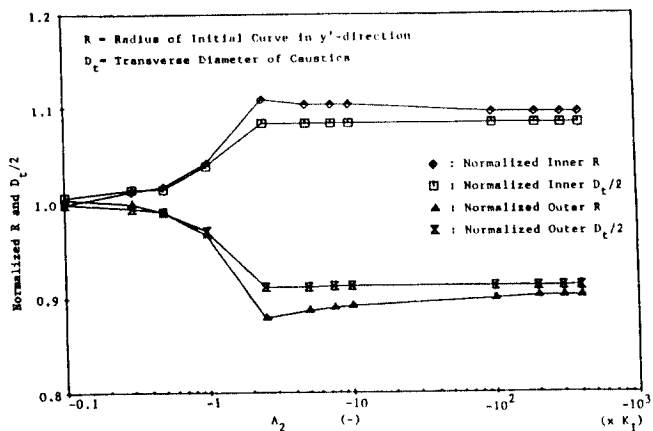
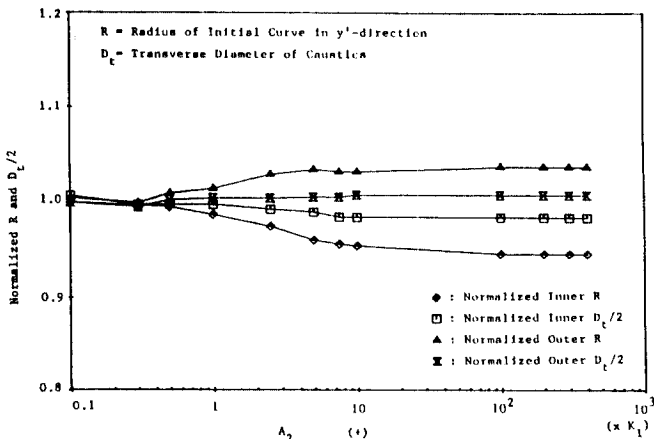


Fig. 3 (b) Theoretically generated Mode II double caustics ( $B_2 = -5K_{II}$ )

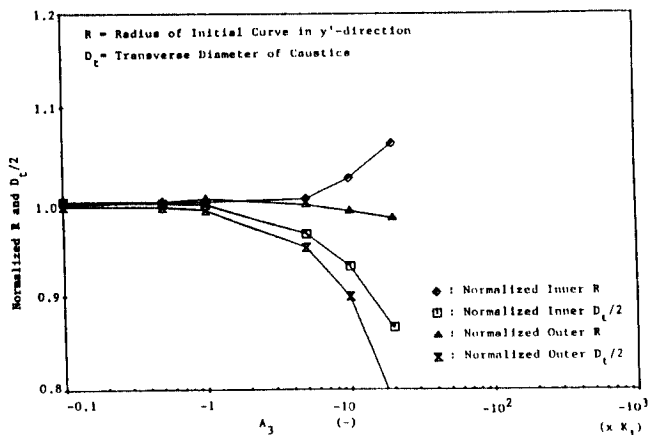


(a)

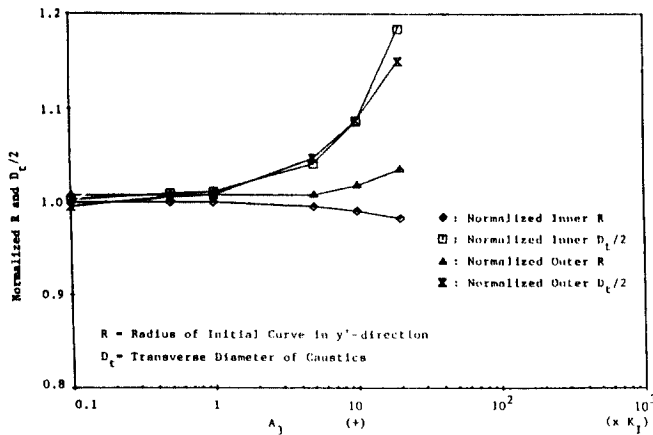


(b)

Fig. 4 (a) (b) Normalized  $R$  and  $D_c/2$  vs. variation of  $A_2$  for Mode I caustics



(a)



(b)

Fig. 5 (a) (b) Normalized  $R$  and  $D_c/2$  vs. variation of  $A_3$  for Mode I caustics

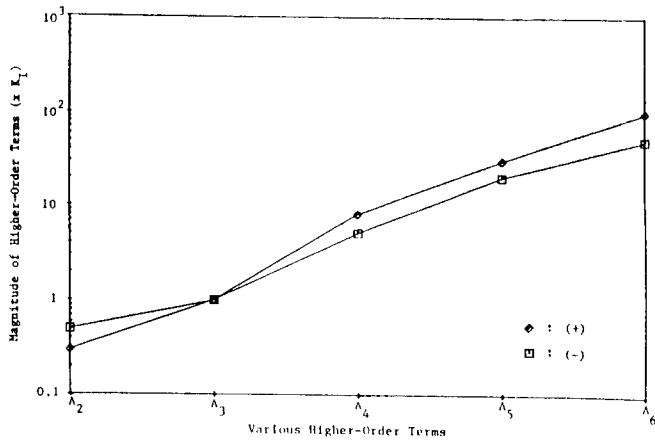


Fig. 6 Lower bound of various higher-order terms affecting shape of caustics(Mode I)

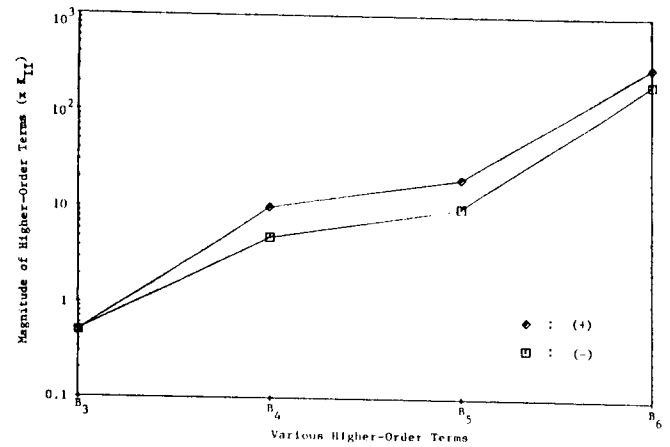
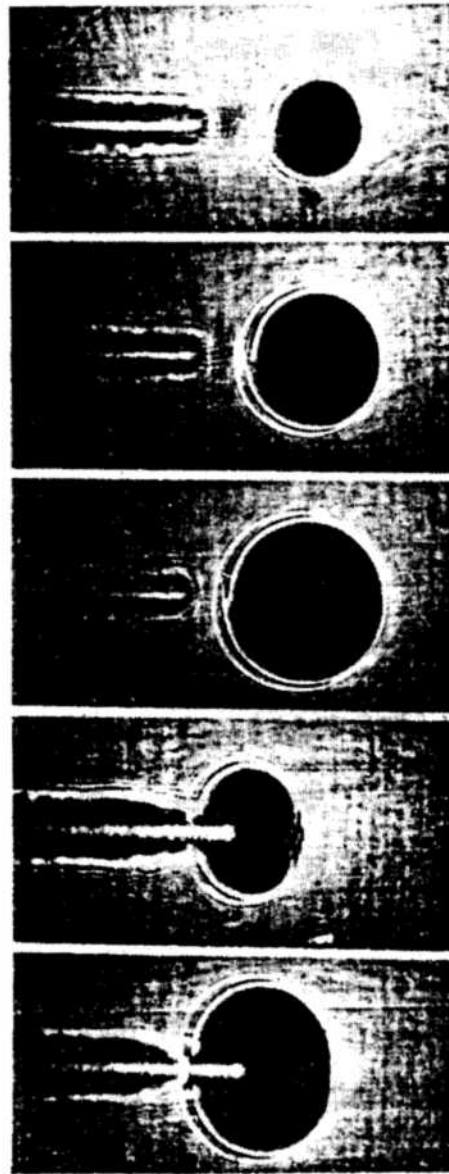
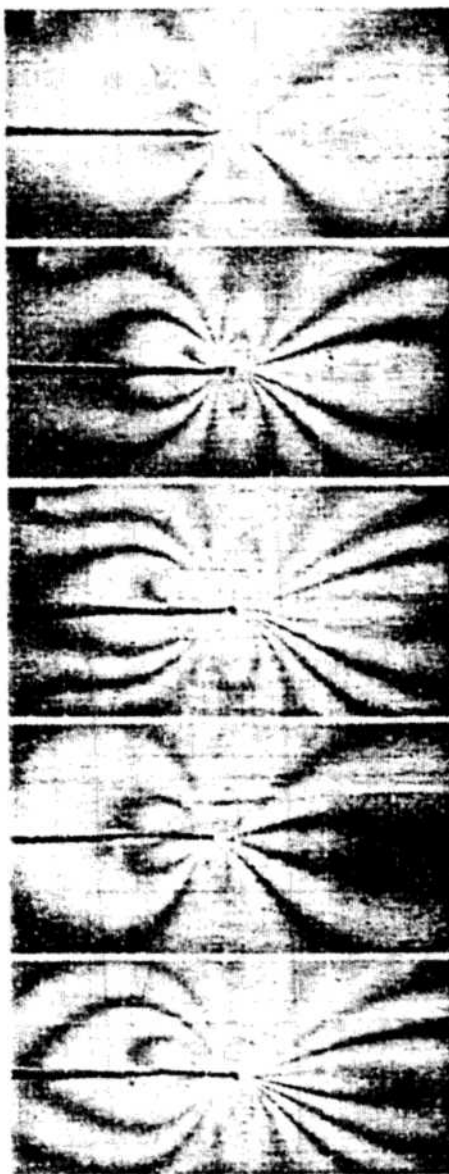


Fig. 7 Lower bound of various higher-order terms affecting shape of caustics(Mode II)



Crack length (mm)	Force $\times 100\text{N}$
36.5	1.02
36.5	2.04
36.5	3.06
55.5	1.02
55.5	2.04

Fig. 8 Variation of shape of caustics with various crack length(PC SEN specimen)

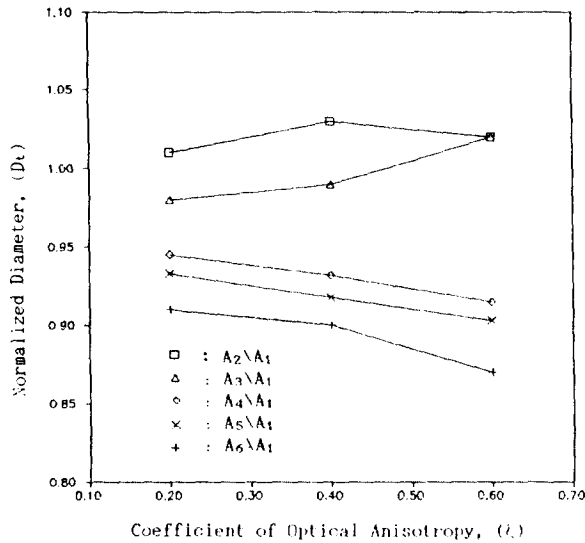


Fig. 9 Normalized transverse diameter( $D_t$ ) w.r.t. reference  $D_t$  vs. optical anisotropy for Mode I inner caustics

various higher-order terms affecting configuration of caustics is shown in Fig. 7. The same compensation phenomenon as that of Mode I loading conditions is found to be appeared in the case of the higher-order terms such as  $B_4$ ,  $B_5$  and  $B_6$ . However, this effect does not occur in the case of  $B_3$ .

Figure 8 shows various caustics in Polycarbonate Single Edge Notch specimens with varying crack lengths under Mode I loading conditions. The experimental set-up for these results may be conferred with Lee(1987). The photoelastic fringe patterns obtained under the same experimental conditions are inserted for reference. It is noted that the shapes of caustics vary according to the crack lengths. The quantitative experimental evaluation of the influence of higher-order terms has yet to be done. However, it is interesting to note that the shape of caustics with the crack length of 55.5mm in Fig. 8 resembles to the theoretically generated caustics shown in Fig. 3(a).

The effect of the higher-order terms and the coefficient of optical anisotropy on the transverse diameter,  $D_t$ , for mode I inner caustics is shown in Figure 9. It is found that the increases in the magnitude of constant term( $A_2$ ) and coefficient of optical anisotropy have the opposite effects on the shape of the caustics within the range of  $1.25 A_1 < A_2 < 12.5 A_1$  with  $\xi = 0.223$  which is for the used Polycarbonate specimens under the plane stress condition.

#### 4. CONCLUDING REMARKS

The effect of the first few higher-order, non-singular stress

terms and the coefficient of optical anisotropy on the shapes of the initial curves and the caustics in birefringent plates under Mode I and Mode II loading conditions was systematically studied by generating both theoretical caustics and initial curves. Theoretically generated caustics with assumed constants was found to be resembled to the experimentally obtained caustics associate with varying crack lengths as far as the shape of caustics is concerned. The methodology for the extraction of more accurate stress intensity factors is expected to be incorporated with the theoretically generated caustics as done in this study including various higher-order terms especially for the crack branching or curving study in optically anisotropic materials. A numerical procedure should be carried out to determine appropriate stress intensity factors and the higher-order terms by using the method of caustics in relatively brittle materials.

#### ACKNOWLEDGEMENTS

The authors wish to acknowledge the financial aid of KOSEF(contract number : 871-0910-004-2) during the course of this investigation.

#### REFERENCES

- Hornbeck, R.W., 1975, "Numerical Methods", Quantum Publishers, INC., pp. 65~66.
- Kalthoff, J.F., 1987, "Shadow Optical Method of Caustics", Handbook on Experimental Mechanics, Society for Experimental Mechanics, pp. 430~500.
- Kobayashi, A.S. and Ramulu, M., 1981, "Dynamic Stress Intensity Factors for Unsymmetric Dynamic Isochromatics", Exp. Mech., 21, 1981, pp. 41~49.
- Lee, O.S. and Kwon, O.K., 1987, "An Experimental Study on Crack Healing of Various Glassy Polymers", KSME Journal, Vol. 1, No. 1, pp. 65~69.
- Phillips, J.W. and Sanford, R.J., 1981, "Effect of Higher-Order Stress Terms on Mode-I Caustics in Birefringent Materials", Fracture Mechanics: Thirteenth Conference, ASTM STP 743, pp. 387~402.
- Theocaris, P.S., and Gdoutos, E.E., 1972, "A Optical Method for Determining Opening-Mode and Edge Sliding-Mode Stress Intensity Factor", J. of Applied Mechanics, Vol. 39, pp. 91~97.
- Theocaris, P.S. and Iokimidis, N.I., 1979, "An Improved Method for the Determination of Mode I Stress Intensity Factors by the Experimental Method of Caustics, J. of Strain Analysis", Vol. 14, pp. 111~118.
- Williams, M.L., 1957, "On the Stress Distribution at the Base of a Stationary Crack", J. of Applied Mechanics, pp. 109~114.